Biologics: Targets and Therapy

Dovepress
open access to scientific and medical research

Open Access Full Text Article

ORIGINAL RESEARCH

New Uracil Analog with Exocyclic Methylidene Group Can Reverse Resistance to Taxol in MCF-7 Cancer Cells

Angelika Długosz-Pokorska[1], Renata Perlikowska[1], Tomasz Janecki[2], Anna Janecka[1]

[1]Department of Biomolecular Chemistry, Faculty of Medicine, Medical University of Lodz, Lodz, Poland; [2]Institute of Organic Chemistry, Faculty of Chemistry, Lodz University of Technology, Lodz, Poland

Correspondence: Angelika Długosz-Pokorska, Department of Biomolecular Chemistry, Medical University of Lodz, Mazowiecka 6/8, Lodz, 92-215, Poland, Tel +48 42 2725706, Fax +48 42 678 42 77, Email angelika.dlugosz@umed.lodz.pl

Introduction: Taxol (Tx), a microtubule-stabilizing drug, has been widely used as a chemotherapeutic in several types of cancer. However, the development of resistance limited its application. One of the strategies used to prevent the emergence of drug resistance is combination treatment, involving at least two drugs. The aim of the current study was to assess if a new uracil analog, 3-*p*-bromophenyl-1-ethyl-5-methylidenedihydrouracil (U-359) can prevent the development of Tx resistance in breast cancer cells.

Methods: The cytotoxicity of the new drug was tested in MCF-7 (hormone receptor (ER, PR) positive cell-line) and MCF-10A cell lines using MTT method. For the detection of apoptosis and necrosis, the Wright and Giemsa staining was used. Gene expression was measured by real-time PCR, and changes in the protein levels were evaluated by ELISA and bioluminescent method.

Results: We investigated the effect of Tx and U-359 on cancer MCF-7 and normal MCF-10A cells alone and in combination. Tx co-administered with U-359 inhibited proliferation of MCF-7 cells to 7% while the level of ATPase drastically decreased to 14%, compared with effects produced by Tx alone. The apoptosis process was induced through the mitochondrial pathway. These effects were not seen in MCF-10A cells, showing the wide safety margin. The obtained results have shown that U-359 produced a synergistic effect with Tx probably by reducing Tx resistance in MCF-7 cells. To elucidate the possible mechanism of resistance, expression of tubulin III (TUBIII), responsible for microtubule stabilization and tau and Nlp proteins, responsible for microtubule dynamics, was assessed.

Conclusion: Combination of Tx with U-359 reduced overexpression of TUBIII and Nlp. Thus, U-359 may stand for a potential reversal agent for the treatment of MDR in cancer cells.

Keywords: MCF-7, MDR, Nlp protein, U-359, taxol, tubulin III

Introduction

Breast cancer is one of the most prevalent malignancies among women in the world.[1] Over the years, various strategies have been developed for the treatment of this cancer type. The most prevalent therapy includes the combination of surgery with chemotherapy. The drugs that show a significant antitumor activity in breast cancer include drugs such as alkylating agents (cyclophosphamide), antimetabolites (methotrexate), anthracyclines (doxorubicin), an orphan antihypertensive drug (Guanabenz acetate) and the mitotic disruptors (taxol).[2–5] Unfortunately, the poor patient response decreases the efficacy of conventional treatment and increases the mortality rate urged for novel cancer therapeutics. For instance, the high therapeutic activity of doxorubicin combined with Ran-RCC1 inhibitory peptide (RAN-IP) in breast cancer has been observed recently. Guanabenz acetate, which was loaded polymersome, has also been an interesting choice for treatment, resulting in a significant decrease in breast tumor size.[2–5]

Nowadays, many medical research studies show that the one of the most effective drugs in the first-line treatment of breast cancer is Taxol, first isolated from the bark of Pacific yew tree (*Taxus brevifolia*) in the 1960s.[2,5] The main mechanism of Tx action is binding to microtubules and inhibiting their disassembly. Cells treated with Tx are arrested in

Received: 17 January 2023
Accepted: 10 April 2023
Published: 15 May 2023

Graphical Abstract

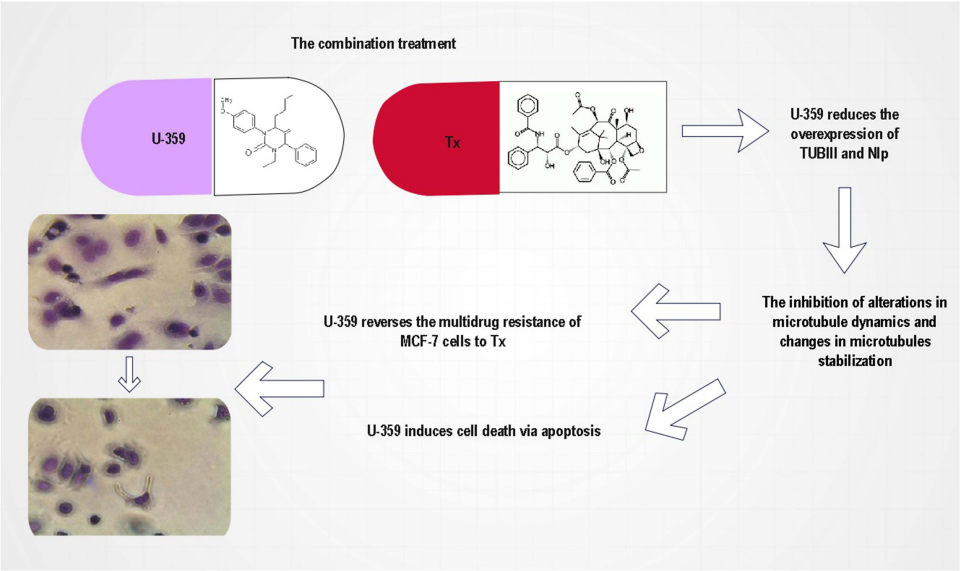

mitosis and eventually undergo death by apoptosis.[6] Unfortunately, cancer cells often develop resistance to Tx which significantly decreases the efficacy of this drug and is a major limitation to its success as a chemotherapeutic agent in fighting cancer.[7–9] The same clinical outcome is associated with high expression of cell proteins such as ABC transporters, tubulins, lysosomal-associated membrane protein in breast cancer or bone morphogenetic protein.[10,11]

Several potential mechanisms of Tx resistance have been proposed. The main one is the overexpression of ABC transporters, in particular multidrug transporter P-glycoprotein/ABCB1, which actively pumps out a wide variety of drugs, including Tx, causing the cells to be resistant to these drugs.[12]

Another potential mechanism of Tx resistance is the modulation of its cellular target, tubulin.[9] Tubulin is a heterodimer formed by α- and β-subunits. Tubulin polymerizes into microtubules which play a crucial role in organization of intracellular structure, intracellular transport, cell division and movement.[6] Tx binds to the microtubule polymer, interfering with the normal function of microtubule breakdown, causing cell death.

The multidrug resistance (MDR) to Tx can develop due to alterations in microtubule dynamics and/or changes in microtubule stabilization. Several studies have reported that the alterations in microtubule dynamics could be caused by altered cellular expression of β-tubulin isotypes, especially *β*III and *β*IV.[13–15]

Recently, two proteins, tau, encoded by *MTBT1* and the ninein-like protein (Nlp), encoded by *NINL* gene, have been considered the most crucial factors engaged in Tx resistance in breast cancer cells. Tau protein plays a significant role in tubulin assembly and polymerization. Several clinical trials have shown the association between Tx and tau binding site in *β*-tubulin, showing that tau protein can act as a Tx competitive inhibitor.[16,17]

Nlp protein is involved in centrosome maturation and spindle formation. It has been found that in women with breast cancer, the higher Nlp expression was correlated with lower sensitivity to Tx chemotherapy.[18]

The development of resistance to Tx in cancer cells started various combination treatments, involving at least two drugs that work by different mechanisms, thereby decreasing the likelihood that resistance will develop. For instance, the high therapeutic activity of taxol combined with fluorouracil in metastatic breast cancer has been reported. In combination treatment, fluorouracil enhanced bioavailability of Tx and showed favorable toxicity profiles supplying more therapeutic way.

Vinorelbine also synergistically improved efficacy of Tx produced a significantly greater proportion of cell kill of cancer p388 murine cells than either drug alone.[19] Two-drug treatment has also played a key role as a determinant of

toxicity and efficacy when taxol and palbociclib are administered to the patients with advanced breast cancer. Dean et al revealed that in breast cancer cells exposed to palbociclib followed by paclitaxel, synergistic reduction in colony formation was noted compared with either drug alone.[20]

Continuing the search for novel compounds with anticancer properties, we recently synthesized a series of uracil analogs combining the uracil skeleton with an *exo*-cyclic methylidene group conjugated with a carbonyl function.[21] The cytotoxic activity of these analogs against two cancer cell lines has been published.[22] They were all highly cytotoxic against MCF-7 cells. In this report, the most potent analog of the series, 3-*p*-bromophenyl-1-ethyl-5-methylidenedihydrouracil (U-359) was selected for combination experiments with Tx. The main goal was to decide if U-359 could act synergistically with Tx in order to down-regulate the level of TUBIII, Nlp and tau proteins responsible, at least in part, for MDR of Tx.

Materials and Methods

Materials

U-359 was synthesized as described elsewhere.[21] Tx was bought from Sigma-Aldrich (St. Louis, MO, USA). For the experiments, U-359 and Tx were dissolved in DMSO and further diluted in culture medium to obtain less than 0.1% DMSO concentration.

Cell Culture

A human breast adenocarcinoma cell line (MCF-7) was bought from the European Collection of Cell Cultures (ECACC). Cells were grown in Minimum Essential Medium Eagle (MEME) having non-essential amino acid solution and antibiotics (100 mg/mL streptomycin and 100 U/mL penicillin, 2 mM glutamine, all obtained from Sigma Aldrich, St. Louis, MO, USA) and 10% fetal bovine serum from Biological Industries (Beit-HaEmek, Israel). A normal human mammary breast cell line (MCF-10A) was bought from the American Type Culture Collection (ATCC). MCF-10A cells were cultured using MEGM Mammary Epithelial Bullet Kit, bought from Lonza (Walkersville, MD, USA). Cells were kept at 37° C in a 5% CO_2 atmosphere and were grown until 80% confluent.

MTT-Assay

The MTT (3-(4,5-dimethylthiazol-2-yl)-2,5 diphenyl tetrazolium bromide) assay, which measures activity of cellular dehydrogenases, was based on the method of Moosmann, and performed as described.[23]

Determination of Cell Morphology Using Light Microscopy

For the detection of apoptosis and necrosis in MCF-7 and MCF-10A cells, the Wright and Giemsa staining (Merck KGaA, Darmstadt, Germany) was used. Giemsa dye stains the cytoplasm of cells orange to pink and nucleus blue to purple, depending on the acidity of the cytoplasmic content.

Briefly, cells were seeded on the 6-well plates (4×10^5 cells/well) and incubated for 24 h with U-359 and/or Tx at IC_{50} concentration each. Untreated cells were served as a negative control. After incubation, the medium was discarded, and cells were fixed in methanol for 5 min. Then, cells were washed with PBS and stained in Wright and Giemsa solution for 30 min. After that, the cells were washed twice with H_2O and left to air-dry. Finally, stained cells were examined using a light microscope and photographed.

Real-Time-Glo MT Cell Viability Assay

To check cell viability of MCF-7 and MCF-10A cells, RealTime-Glo™ MT (RTG MT) assay (Promega, Mannheim, Germany) was performed according to the standard protocol. Briefly, MCF-7 and MCF-10A cells were seeded on 96-well plates at a density 0.5×10^4/mL in 50 µL standard growth medium and incubated for 24 h with U-359 and/or Tx at IC_{50} concentration each. After incubation, 50 µL of 2x RealTime-Glo reagent was added to each well. Then, the plate was incubated for 1 h at 37°C in a humidified incubator. The intensity of the luminescence signal was measured using

Flexstation 3. The effect of the combination treatment was compared with those produced by the tested compounds alone.

ApoSENSOR Cell Viability Assay Kit

ATPase activity in MCF-7 and MCF-10A cells incubated with U-359 and/or Tx was measured by a bioluminescent method (ApoSENSOR Cell viability assay kit (Bio Vision, Inc. Headquarters, California, USA), according to the standard protocol. Briefly, MCF-7 and MCF-10A cells were seeded on 96-well plates at a density 10^4/mL in 100 µL standard growth medium and incubated with the tested compounds (U-359; Tx) or co-incubated with U-359+Tx (at IC_{50} concentration each) for 24 h. Then, culture medium was removed and 100 µL of Nucleotide Releasing Buffer was added to each well. The plate was gently shaken for 5 min at RT. The effects of the combination treatment were compared with those produced by the tested compounds alone.

Real-Time Assessment of Cell Death Type

Cell death type was found using the RealTime-GloTM Annexin V Apoptosis and Necrosis Assay (Promega, Mannheim, Germany), according to the manufacturer's guidelines. The test kit included Annexin V-LgBiT (1,000X), Annexin V-SmBiT (1,000X), CaCl2 (1,000X), Annexin V NanoBiT® Substrate (1,000X), Necrosis Detection Reagent (1,000X). Briefly, MCF-7 cells were seeded on 96-well plates at a density 1.0×10^4/mL in 50 µL of the standard growth medium and incubated for 24 h with U-359 and/or Tx at IC_{50} concentration each. After incubation, 100 µL of 2× detection reagent was added to each well. Then, the plate was shaken for 30 seconds (at 500–700 rpm) and incubated in a humidified incubator. The luminescence signal and fluorescence intensity were analyzed using Flexstation 3. The effects of the combination treatment were compared with those produced by the tested compounds alone.

Assessment of Human PARP1 Protein Levels by ELISA-Based Method

The PARP1 protein level in MCF-7 cells incubated with the tested compounds was measured by the ELISA-based method using Cleaved PARP1 Human Simple Step ELISA® Kit (ABCAM, Cambridge, UK). Briefly, cells were seeded on the 6-well plates (4×10^5 cells/well) and incubated for 24 h with U-359 and/or Tx at IC_{50} concentration each. After incubation, growth medium was removed and cold 1X Cell Extraction Buffer PTR was added directly to the plate. Then, cells were harvested and incubated on ice for 15 min. The cellular lysates were centrifuged at 18,000 × g for 20 min at 4°C. Properly diluted protein extracts (25 µg) and standards were added into each well of 96-well plates pre-coated with anti-cleaved PARP1-specific antibodies. PARP1 cleaved by activated caspase-3 between Asp214 and Gly215 was bound to the wells by immobilized antibodies. Addition of a secondary antibody conjugated to horseradish peroxidase (HRP) supplied sensitive colorimetric readout. Finally, the stop solution was added to each well. The optical density (OD) of the yellow solution was measured spectrometrically at the 450 nm wavelength.

The Caspase-Glo® 8 and 9 Assay

The caspase 8 and 9 activation in MCF-7 cells was detected, using a luminometric assay kit (Caspase-Glo 8 and 9; Promega, Mannheim, Germany) according to the manufacturer guidelines. The assay supplies the luminescent caspase 8 and 9 reagents that have the sequences cleaved to release luminescence signals. Briefly, MCF-7 cells were seeded on 96-well plates at a density 2×10^4/mL in 100 µL of the standard culture medium and left to grown for 24 h. Then, the tested compounds (U-359 and/or Tx) at IC_{50} concentration were added to each well and incubated for 24 h. After incubation, Caspase-Glo® Reagents were added. Finally, the plate was gently mixed for 2 min, incubated for 30 min at RT and read within 2 min in the Flexstation 3. The effects of the combination treatment were compared with those produced by the tested compounds alone.

Quantitative Real-Time PCR Assay

The mRNA levels of *MTBT1* and *NINL* genes were analyzed by quantitative RT-PCR. Briefly, MCF-7 cells were seeded on the 6-well plates at the proper cell density (4.0×10^5 cells/well) and incubated. Then, MCF-7 cells were incubated for 24 h with U-359 and/or Tx at IC_{50} concentration each. The effect of the combination treatment was compared with those

produced by the tested compounds alone. Total RNA was extracted using the Total RNA Mini Kit (A&A Biotechnology, Gdynia, Poland) according to the manufacturer protocol. The concentration of RNA was measured using sensitive single-tube fluorimeter for fluorescence-based quantitation of nucleic acids and proteins. The concentration used for further experiments was always 150 ng/μL. TranScriba Kit (A&A Biotechnology, Gdynia, Poland) was used for cDNA synthesis. Amplification of gene-specific primers (Table 1) was performed using Real-Time 2x-PCR SYBR Master Mix (A&A Biotechnology, Gdynia, Poland) in Stratagene MX3005P QPCR System (Agilent Technologies, Inc. Santa Clara, CA, USA) according to the manufacturer's instructions. GAPDH was used as an internal reference gene to normalize the expression of investigated genes. The expression levels of the tested genes were figured out by the $2^{-\Delta\Delta CT}$ method.[24]

Human TUBβ3 (Tubulin Beta 3) ELISA Kit

The Tubulin Beta 3(TUBβ3) protein levels in MCF-7 cells incubated with the tested compounds were measured by the ELISA-based method using Human TUBβ3 (Tubulin Beta 3) ELISA Kit.

Briefly, cells were seeded on the 6-well plates (density 4.0×10^5 cells/well) and incubated with U-359/Tx or co-incubated (U-359+Tx) for 24 h. The cells were washed with PBS and collected by centrifugation at 1000×g for 5 min. Protein extracts were prepared using lysis buffer and ultrasonication. Then, 20 μg of protein extracts and properly diluted standards were added into each well of 96-well plates pre-coated with TUBβ3 specific antibodies. Tubulin Beta 3 protein is present in the prepared extracts specifically bound to the wells by immobilized antibodies. Addition of the streptavidin-HRP solution supplied sensitive colorimetric readout. Finally, the stop solution was added to each well. The optical density (OD) of the yellow solution was measured spectrometrically at the 450 nm wavelength.

Human Ninein-Like Protein (Nlp) ELISA Kit

The Nlp protein level in MCF-7 cells incubated with the tested compounds was assessed by the human ninein-like protein (Nlp) kit (Abbexa LTD, Cambridge, UK). Briefly, cells were seeded on the 6-well plates (4×10^5 cells/well) and incubated with U-359 and/or Tx (at IC_{50} concentration each) for 24 h. Then, cells were washed with PBS and collected by centrifugation at 1500×g for 10 min at 2–8°C to remove cellular debris. Properly diluted protein extracts (25 μg) and standards were added into each well of 96-well plates pre-coated with anti-Nlp specific antibodies. These proteins are present in the prepared extracts specifically bound to the wells by immobilized antibodies. The addition of a secondary antibody conjugated to horseradish peroxidase (HRP) supplied sensitive colorimetric readout. Finally, the stop solution was added to each well. The optical density (OD) of the yellow solution was measured spectrometrically at the 450 nm wavelength.

Statistical Analysis

Statistical analysis was performed using Prism 6.0 (GraphPad Software Inc., San Diego, CA, USA). Results from at least three independent experiments in triplicate were expressed as mean±SEM. Statistical significance was analyzed using one-way ANOVA followed by a post hoc multiple comparison Student–Newman–Keuls test, *p<0.05, **p<0.01, and ***p<0.001 was considered statistically significant.

Table 1 Primer Sequences for RT-PCR

Gene	Primer Sequences	
	Forward Primer	**Reverse Primer**
GAPDH	GTCGCTGTTGAAGTCAGAGGAG	CGTGTCAGTGGTGGACCTGAC
MTBT1	AGCAACGTCCAGTCCAAGT	TCTGTCCTTGAAGTCCAGCT
NINL	TTTGCTCGAGCGATGCTTGTGTCCG	GACAGGATCCTTGAGGCGGTTACTG

Results

Chemical Synthesis

U-359 was synthesized by reduction of carbon–carbon double bond in 5-diethoxyphosphoryldihydrouracils **1**, followed by Horner–Wadsworth Emmons olefination of formaldehyde using dihydrouracils **2** (Scheme 1).

MTT-Assay

The cytotoxicity of U-359 was evaluated in tumor MCF-7 cells and in MCF-10A normal cells using the standard MTT-assay, which is based upon the ability of viable cells to metabolically reduce yellow water-soluble tetrazolium salt into non-soluble purple formazan product. Cells were exposed to a broad range of compound concentrations for 24 h. In MCF-7 cells, Tx showed cytotoxic activity with IC_{50} value 0.5 μM but U-359 showed high cytotoxic activity with IC_{50} value 3.8 μM and about threefold selectivity as compared with normal MCF-10A cells (IC_{50} value 13 μM) (Figure 1).

Real-Time-Glo MT Cell Viability Assay

To assess the number of MCF-7 and MCF-10A cells with reduced potential, RealTime-GLO MT Cell Viability Assay was used. All cells were incubated for 24 h with U-359 and/or Tx at IC_{50} concentration each. Healthy cells reduce the proprietary pro-substrate to generate a substrate for NanoLuc® luciferase that can diffuse from cells into the culture medium. Then, it is rapidly used by the NanoLuc® Enzyme to produce a luminescent signal which correlates with the number of viable cells. The luciferase enzyme (NanoBiT™) produces no luminescence in healthy cells. The early

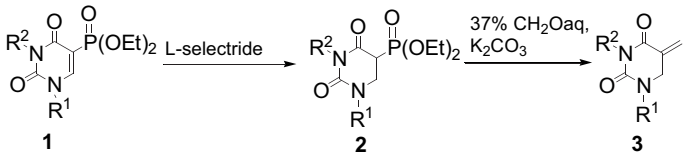

Scheme 1 Synthesis of 1-ethyl-3-*p*-bromophenyl-5-methylidenedihydrouracil (U-359).

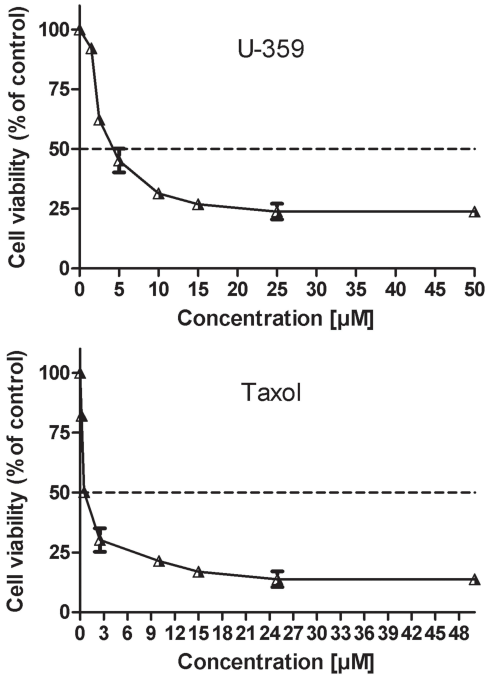

Figure 1 The cytotoxic effect of U-359 and Tx on MCF-7 cells was analyzed by MTT assay. The IC_{50} value was estimated using the fitted line, Y = a * X + b, IC_{50} = (0.5 - b)/a.

apoptosis is detected when the level of luminescence increases, while necrosis is correlated with up-regulation of fluorescence signal.

As shown in Figure 2, Tx decreased luminescence signal in MCF-7 cell, down to 49%, while the RLU signal produced by U-359 decreased to 3%. Co-incubation U-359 and Tx potently down-regulated the level of RLU, to 7%, compared with effects produced by Tx alone. By contrast, incubation of MCF-10A with Tx or co-incubation with U-359 +Tx led to only a modest decrease (20%) in the number of viable cells (Figure 2).

The Metabolic Function of MCF-7 Cells

The metabolic functions of cells require the proper amount of energy from ATP hydrolysis. As ATP level falls to a point where the cell can no longer perform basic functions, the cell dies. Therefore, decrease in ATP level can be used as an indicator of cell death.

To assess the level of ATP in MCF-7 and MCF-10A cells, ApoSENSOR™ Cell Viability Assay Kit was used. All cells were incubated for 24 h with U-359 and/or Tx at IC_{50} concentration each. As shown in Figure 2, in MCF-7 cell line, U-359 and Tx reduced the activity of ATPase by 90% and 52%, respectively. In a two-drug combination experiment (U-359+Tx), the level of ATPase in MCF-7 cells drastically decreased to 14%. In MCF-10A, Tx reduced the activity of ATPase only by 15%, while co-incubation with U-359 and Tx caused an increase in ATPase activity (up to 10%), compared with effect produced by Tx alone. On the other hand, in MCF-10A, the effect produced by U-359 was not significant (Figure 2).

Determination of Cell Morphology Using Light Microscopy

The morphological changes of MCF-7 and MCF-10A cells incubated for 24 h with U-359 and/or Tx (at IC_{50} concentration each) were observed using Wright's Giemsa staining. Morphological analysis showed that the cells in

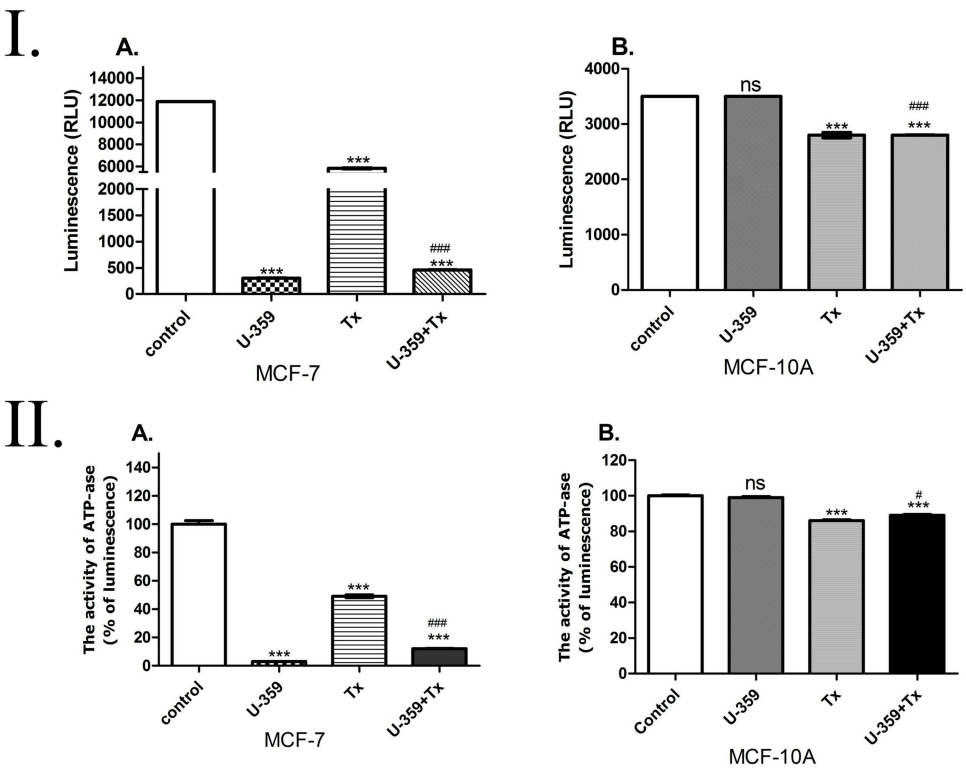

Figure 2 (**I**) Real-time monitoring of the number of MCF-7 (**A**) and MCF-10A (**B**) cells with reduced potential and metabolism expressed as the level of luminescence (RLU) measured for the U-359, Tx and U-359+Tx. Untreated MCF-7 cells were used as a control. Data are expressed as mean ± SEM. Statistical significance was assessed using one-way ANOVA and a post hoc multiple comparison Student–Newman–Keuls test. $^{***}p$ <0.001 (statistical significance), in comparison with control; $^{\#\#\#}p$ <0.001 (statistical significance), in comparison with Tx. (**II**) The activity of ATPase in MCF-7 (**A**) and MCF-10A (**B**) cells measured as the level of luminescence signal (RLU) measured for the U-359, Tx and U-359+Tx. Untreated MCF-7 cells were used as a control. Data are expressed as mean ± SEM. Statistical significance was assessed using one-way ANOVA and a post hoc multiple comparison Student–Newman–Keuls test. $^{***}p$ <0.001, in comparison with control; $^{\#\#\#}p$ <0.001; $^{\#}p$ <0.05 ((statistical significance), in comparison with Tx; ns (no significant).

the control group had normal morphology, while U-359 and Tx treatment caused the enlargement of cells, chromatin condensation and nuclear fragmentation. Additionally, U-359 induced the formation of small apoptotic bodies (Figure 3). In the combination experiment (U-359+Tx), the number of cells with all apoptotic features was greatly

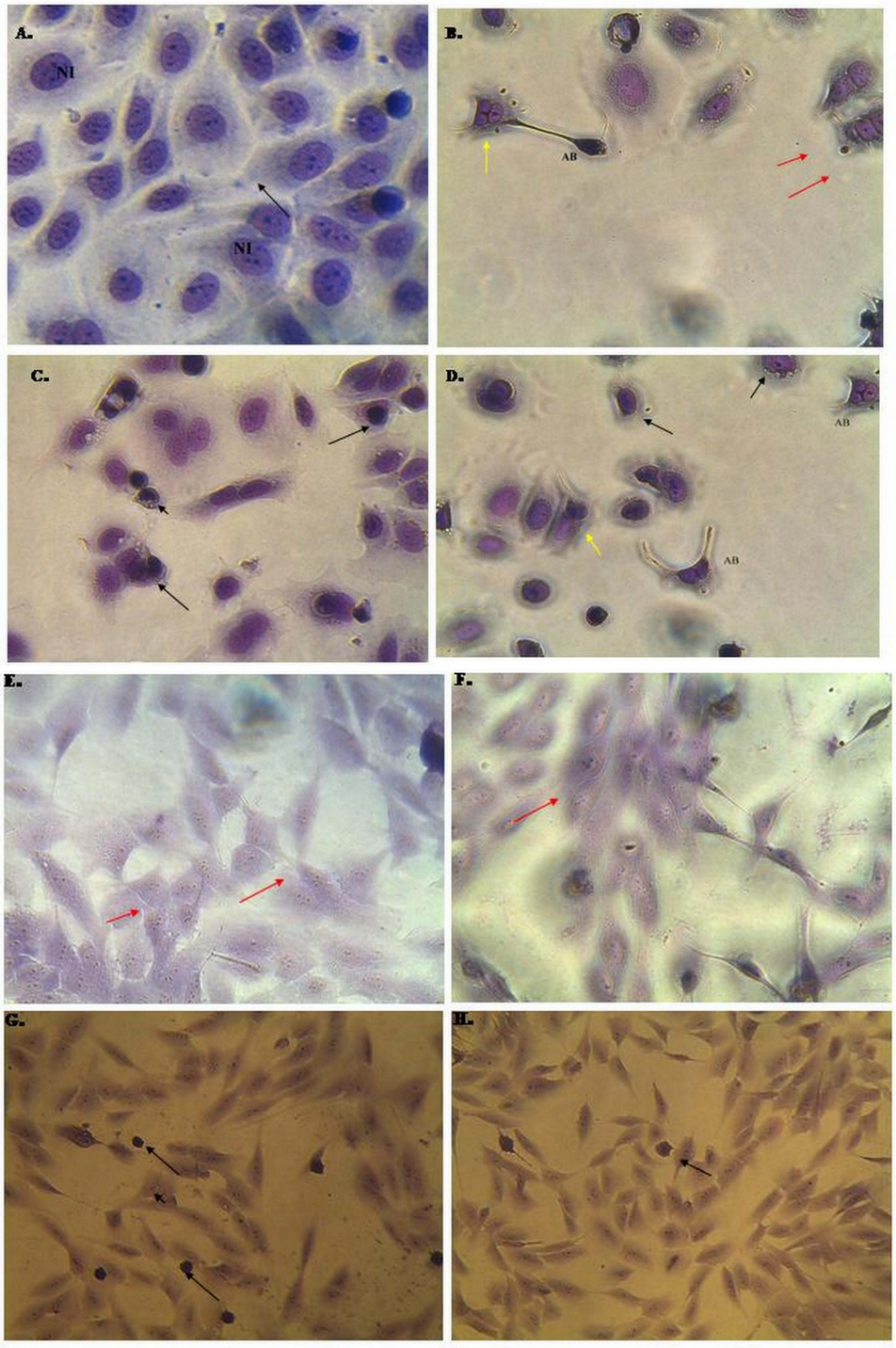

Figure 3 Effect of U-359, Tx and U-359+Tx on the morphology of MCF-7 and MCF10A cells after 24 h incubation. (**A**) The untreated MCF-7 cells (control) are marked by black arrows – normal angular or polygonal shape, large vesicular nucleus, and prominent nucleolus; Nl – nucleoli (**B**) MCF-7 cells treated with U-359 are marked with red arrows - chromatin condensation; yellow arrows- cytoplasm and chromatin condensation; AB – the apoptotic body (**C**) MCF-7 cells treated with Tx: black arrows shrunken cytoplasm and chromatin condensation. (**D**) MCF-7 cells treated with U-359+Tx: black arrows- shrunken cytoplasm and chromatin condensation; AB – the apoptotic body; yellow arrows – cytoplasm and chromatin condensation, nuclear fragmentation. (**E**) Morphology of untreated MCF-10A; (**F**) U-359: red arrows – normal angular or polygonal shape, large vesicular nucleus, and prominent nucleolus; (**G**) Tx; (**H**) U-359+Tx: black arrows-abnormal morphology, cytoplasm, and chromatin condensation.

increased. As shown in Figure 3 in MCF-10A cells treated with U-359 the apoptotic changes have not been observed. All cells had normal morphology as compared to the MCF-10A untreated cells. The abnormal morphology was observed in these cells incubated with Tx, while co-incubation with U-359 and Tx did not show significant changes (Figure 3).

Induction of Apoptosis

Real-Time Assessment of Cell Death Type

To find the type of MCF-7 cell death, RealTime-GloTM Annexin V Apoptosis and Necrosis Assay was used. Apoptosis (translocation of phosphatidylserine to the outer part of the cell membrane) can be detected by luminescence, while necrosis (translocation of phosphatidylserine on the inner and outer part of the cell membrane) by fluorescence. Increases of both luminescence and fluorescence signals are characteristic for the loss of membrane integrity (secondary necrosis following apoptosis). On the other hand, positive luminescence and negative fluorescence signals reflect early apoptosis (Annexin V binding).

MCF-7 cells were incubated for 24 h with U-359 or Tx alone or co-incubated with U-359+Tx.

As shown in Figure 4A and B, U-359 and Tx both increased the level of RLU (luminescence signal) by 19% and 4%, respectively, and RFU (fluorescence signal) by 135% and 8%, respectively, which points at the late apoptosis. Co-incubation of MCF-7 cells with U-359 + Tx caused a significant increase in the fluorescence signal, by 24% and luminescence signal by 42%, compared with the effects produced by Tx alone. The obtained results showed a significant difference between luminescence and fluorescence kinetic effects in MCF-7 cells incubated with U-359 and co-incubated with U-359 and Tx. In all tested samples, a considerable time delay between increase of luminescence and fluorescence signals was seen, which confirmed a late apoptosis leading to secondary necrosis (Figure 4C and D).

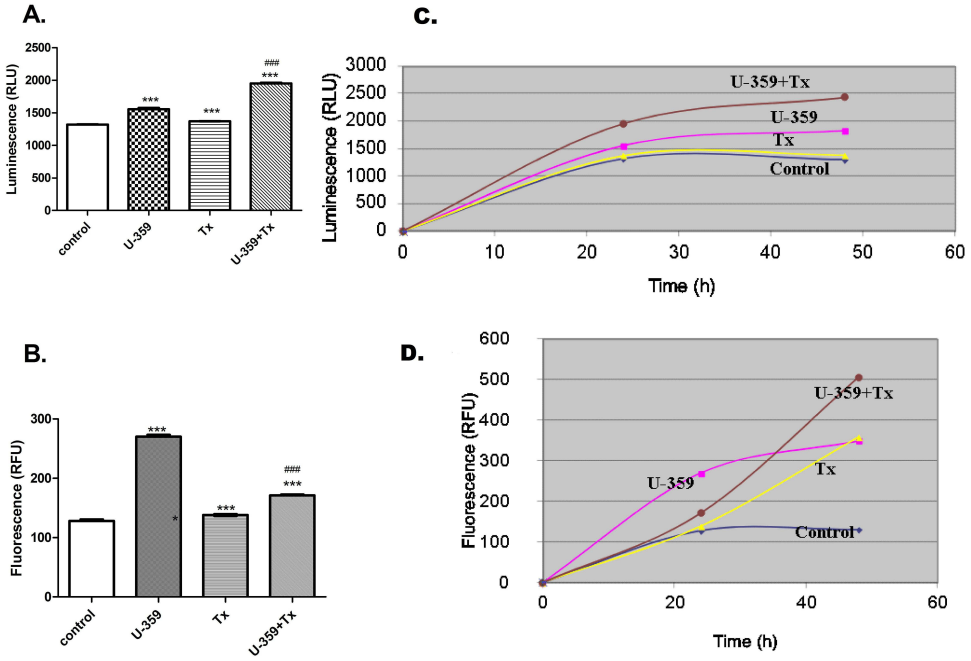

Figure 4 Real-time monitoring of luminescence RLU (**A**) and fluorescence RFU (**B**) signals measured for the U-359, Tx and U-359 + Tx experiments. Untreated MCF-7 cells were used as a control. The time-course dependent luminescence (**C**) and fluorescence (**D**) measurement. The detection of apoptosis and necrosis process in MCF-7 cells incubated with U-359 or Tx, compared with combination experiments (U-359+Tx). The intensity of luminescence and fluorescence signals were measured after 1, 24 and 48 h. Data are expressed as mean ± SEM. Statistical significance was assessed using one-way ANOVA and a post hoc multiple comparison Student–Newman–Keuls test. ***p <0.001 (statistical significance), in comparison with control; ###p <0.001 (statistical significance), in comparison with Tx.

https://doi.org/10.2147/BTT.S405080 DovePress

Assessment of Human PARP1 Protein Level by ELISA-Based Method

Apoptosis in MCF-7 cells was evaluated using Cleaved PARP1 Human SimpleStep ELISA® Kit. MCF-7 cells were incubated with U-359/Tx or co-incubated for 24 h. Poly ADP-ribose polymerase 1 (PARP1) is a DNA repair enzyme that in apoptosis is cleaved by activated caspases. Therefore, the 89-kDa PARP1 is a hallmark of apoptosis.

As shown in Figure 4, MCF-7 incubated with U-359 showed an increase in the level of cleaved PARP1, by 123%, while Tx enhanced the amount of PARP1 fragment only by 17%. In combination experiment, the level of 89 kDa PARP1 increased up to 83%, compared with the effect produced by Tx alone (Figure 5).

The Caspase 8 and 9 Activity

Caspase 8 plays a key role in the extrinsic-mediated apoptotic pathway, while caspase 9 is necessary to remodel the mitochondria during intrinsic pathway. To measure the caspase 8 and 9 activity in MCF-7 cells, a luminometric assay was used.

MCF-7 cells were incubated for 24 h with U-359 and/or Tx (at IC_{50} concentration each). U-359 significantly increased the level of caspase 9 and did not activate caspase 8. Tx decreased the activity of both proteins. Co-incubation of MCF-7 cells with U-359 and Tx caused a significant increase of caspase-9 activity, compared with the effect produced by Tx alone (Figure 6).

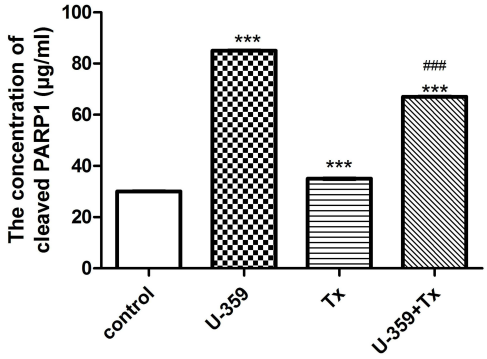

Figure 5 The concentration of cleaved PARP1 in MCF-7 cells. Protein extracts from MCF-7 cells obtained after treatment with U-359/Tx/U-359+Tx (at IC_{50} concentrations) were tested by the ELISA-based method using Cleaved PARP1 Human SimpleStep ELISA® Kit. Data are expressed as mean ± SEM. Statistical significance was assessed using one-way ANOVA and a *post-hoc* multiple comparison Student–Newman–Keuls test. ***p <0.001 (statistical significance), in comparison with control; ###p <0.001 (statistical significance), in comparison with Tx.

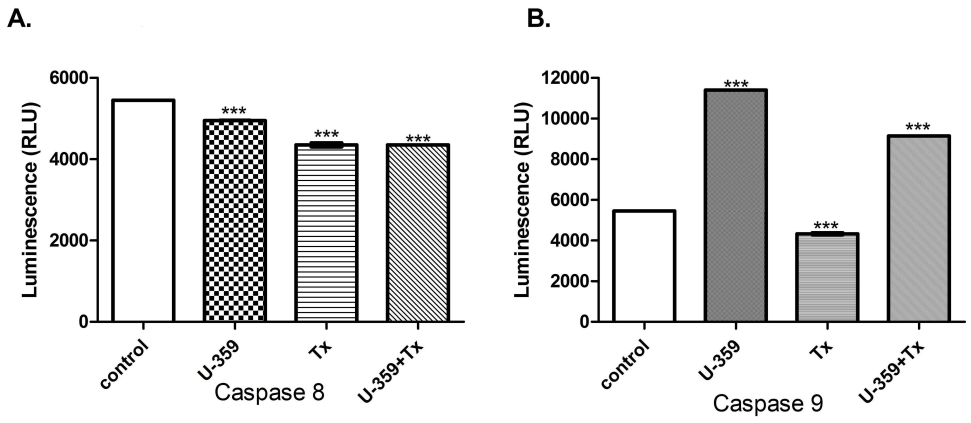

Figure 6 Determination of caspase 8 (**A**) and 9 (**B**) activity. The luminescence signals (RLU) measured for the U-359, Tx and combination experiment (U-359+Tx). Untreated MCF-7 cells were used as a control. Data are expressed as mean ± SEM. Statistical significance was assessed using one-way ANOVA and a *post-hoc* multiple comparison Student–Newman–Keuls test. ***p <0.001 (statistical significance), in comparison with control.

The Possible Mechanism of Multidrug Resistance of MCF-7 Cells to Tx

Quantitative Real-Time PCR Assay

The mRNA expression of *MTBT1* and *NINL* genes in MCF-7 cells incubated with U-359, Tx or co-incubated for 24 h with both compounds was assessed by real-time PCR.

The treatment of the cells with either U-359, Tx or both compounds together did not affect *MTBT1* expression (Figure 6). U-359 used alone decreased the mRNA level of *NINL*, while Tx alone increased the expression of this gene. However, the co-incubation of both compounds caused a significant down-regulation of *NINL* (Figure 7).

The Alterations in Microtubule Dynamic

Human TUBIII Assay

The concentration of TUBIII was found in MCF-7 by Human TUBbetaIII (Tubulin Beta 3) ELISA Kit. Tubulin beta 3 monoclonal antibodies recognized beta tubulin class III. In the presence of microtubule disrupter, such as Tx, unstable polymers made of III-tubulin are formed that may be considered markers of resistance.

Tx significantly increased the level of TUBIII in MCF-7 cells. The opposite effect was produced by U-359, which caused a twofold decrease of this protein concentration. In the combination experiment, U-359+Tx inhibited protein expression almost completely, as compared with the effects produced by Tx alone (Figure 8A).

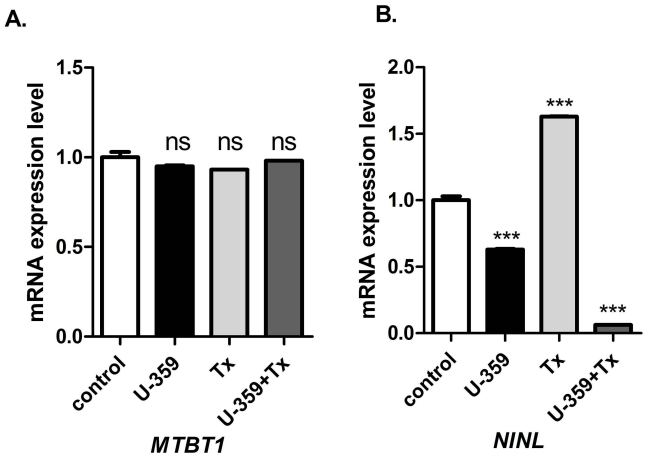

Figure 7 Real-time PCR analysis of *MTBT1* (**A**) and *NINL* (**B**) expression in MCF-7 cells treated with U-359, Tx and U-359+Tx. Data are expressed as mean ± SEM. Statistical significance was assessed using one-way ANOVA and a post hoc multiple comparison Student–Newman–Keuls test. *** p <0.001 (statistical significance), In comparison with control.

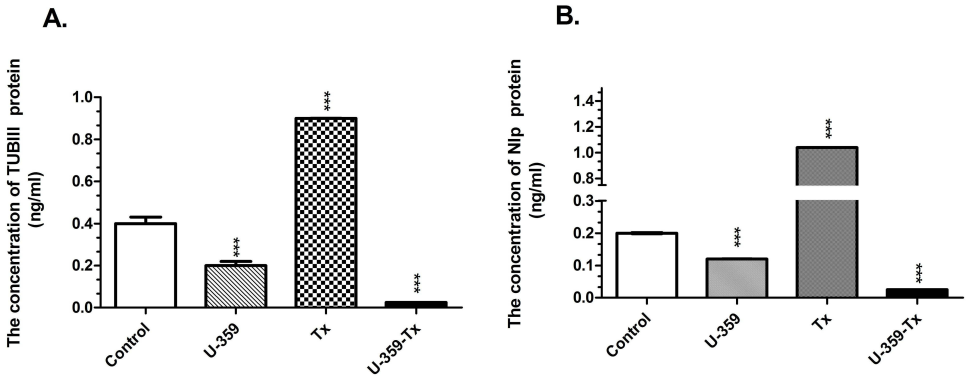

Figure 8 Protein level of TUBIII (**A**) and Nlp (**B**) in MCF-7 cells treated with U-359, Tx and U-359+Tx. Data are presented as mean±SEM. Statistical significance was assessed by the Student's *t*-test ***$p<0.001$ (statistical significance), in comparison with control.

The Quantitative Detection of Nlp Protein

To measure Nlp protein concentration in cancer cell lysates, Human Ninein-Like Protein (Nlp) ELISA Kit was used. Cell lysates were prepared after incubation of MCF-7 cells with U-359 and/or Tx for 24 h.

Consistent with enhanced gene expression, Tx significantly up-regulated, while U-359 alone and in combination with Tx potently down-regulated the level of Nlp (Figure 8B).

Discussion

Combination chemotherapy, the simultaneous administration of two or more drugs, may supply several advantages over monotherapy, such as better efficacy, dose reduction, decreased toxicity, and reduced development of drug resistance.[25] Due to these advantages, combination chemotherapy is now an often-used strategy in cancer treatment, including breast cancer.[26,27] Tx shows a substantial single-agent activity in metastatic breast cancer, but the main problem with its use is the development of resistance. Administration of Tx together with other anticancer agents may be a good strategy to reverse MDR of this drug and to improve its therapeutic efficacy. In some clinical trials Tx was successfully administered with 5-fluorouracil, vinorelbine and doxorubicin.[19]

Several in vitro studies were performed in the search for agents capable of reversing MDR of Tx. A synthetic drug, ponatinib, significantly enhanced the accumulation of Tx in breast cancer cells overexpressing ABCC10/MRP7 transporter, downregulating MRP7 protein expression in a time- and concentration-dependent manner. Thus, ponatinib may be a potential reversal agent for the treatment of MDR.[28]

Piperine, alkaloid isolated from black pepper, improved the bioavailability and antitumor effect of Tx in MCF-7 cells.[29] Rapamycin also synergistically improved the efficacy of Tx in the multidrug resistant MCF-7/ADR breast cancer cells.[30]

NSC23925, a selective P-glycoprotein (Pgp) inhibitor, in combination with Tx was shown to produce a significant efficiency in preventing the emergence of MDR in breast cancer cells.[31]

Here, we investigated the in vitro anticancer activity of a novel synthetic uracil analog **U-359**. The study was performed on the breast cancer MCF-7 cell line and, for comparison, on non-malignant breast epithelial MCF-10A cell line. **U-359** turned out to be threefold less cytotoxic against MCF-10A than MCF-7 cells.

To explore the anticancer activity and safety of **U-359** in combination with Tx, monitoring of the MCF-7 and MCF-10A cell viability was performed. Proliferation of MCF-7 cells was significantly inhibited when Tx was co-incubated with **U-359**, MCF-10A cells were affected only in a ridiculously small percentage. This result was further confirmed by assessing ATPase activity which was greatly decreased in the combination experiment in MCF-7, but not in MCF-10A cells. Morphological changes typical for apoptosis were seen in MCF-7 cells treated with Tx or with **U-359**. In the combination experiment (**U-359**+Tx), the number of cells with all apoptotic features increased drastically. MCF-10A cells treated with **U-359** and **U-359**+Tx, but not Tx alone, had normal morphology.

As opposed to Tx alone, which moderately induced apoptosis in cancer cells, the effect observed in the MCF-7 cells co-incubated with Tx and **U-359** was extraordinarily strong. Also, the level of PARP1, a hallmark of apoptosis, increased significantly in co-incubation treatment. Further experiments were performed to assess the level of caspase 8 and 9.

Considering the high anticancer activity of Tx in combination with **U-359**, as compared with Tx alone, we hypothesized that **U-359** may reduce resistance of MCF-7 cells to Tx. To elucidate the possible mechanism of drug resistance in MCF-7 cells, the mechanism of alterations in microtubule dynamics and/or changes in microtubule stabilization was analyzed. The quantitative analysis of the mRNA expression of *MTBT1* and *NINL*, two key genes engaged in Tx resistance, was performed. Real-time PCR experiments indicated that Tx used alone did not affect *MTBT1* but enhanced the mRNA level of *NINL*, while **U-359** had the opposite effect. In combination experiments, significant down-regulation of *NINL* expression was observed. Consistent with gene expression, Tx in combination with **U-359** significantly decreased the protein level of Nlp (by 85%) in MCF-7 cells. Given the fact that the alterations in microtubule dynamics could be caused by expression of modified beta-tubulin III, the level of TUBIII protein was measured. The obtained results indicated that **Tx+U-359** decreased the level of TUBIII almost completely (by 88%), as compared with the effect produced by Tx (an increase in the level of cleaved TUBIII by 125%) alone (Figure 9).

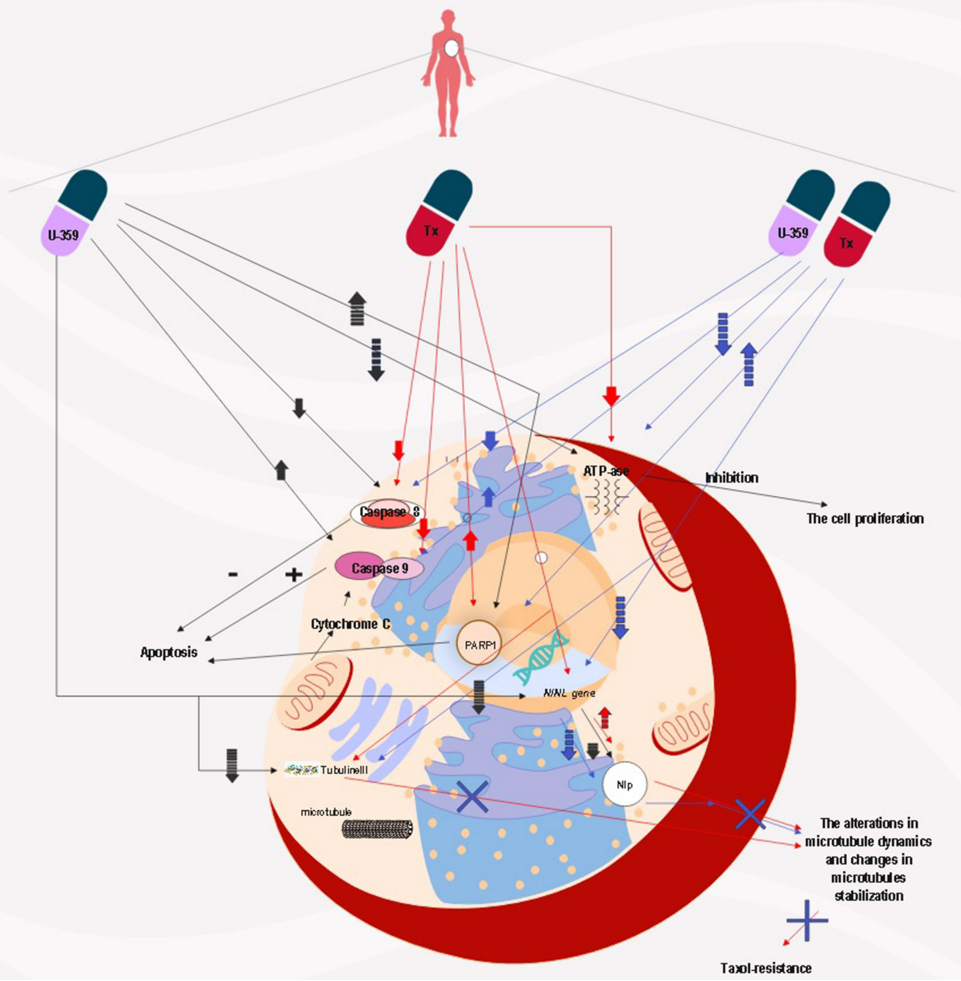

Figure 9 The possible response mechanism of U-359 in the Tx resistance of MCF-7 cells.

Conclusion

The development of taxol resistance limited its application. One of the strategies used to prevent the emergence of drug resistance is combination treatment, involving at least two drugs.

Continuing the search for novel compounds with anticancer properties, a new uracil analog, 3-*p*-bromophenyl-1-ethyl-5-methylidenedihydrouracil (U-359) was synthesized. The aim of the current study was to assess if U-359 can prevent the development of Tx resistance in breast cancer cells. U-359 exhibited a broad spectrum of anti-proliferative activities against the tested cancer cell lines. Apoptosis studies against MCF-7 cells showed that apoptosis induction went through the mitochondrial pathway. Considering the high anticancer activity of Tx in combination with **U-359**, as compared with Tx alone, it was hypothesized that **U-359** may reduce resistance of MCF-7 cells to Tx. To elucidate the possible mechanism of resistance, expression of tubulin III (TUBIII), responsible for microtubule stabilization and Nlp proteins, responsible for microtubule dynamics, was assessed. Tx in combination with **U-359** significantly decreased the level of both proteins. Based on the obtained results, it can be concluded that **U-359** shows significant synergistic effect in combination with Tx and prevents the development of Tx resistance in MCF-7 cells causing alterations in microtubule dynamics and changes in microtubules' stabilization (Figure 9) Consequently, this uracil analog has a potential as a promising anticancer agent able to overcome MDR in breast cancer cells and appears to be a suitable candidate for the future in vivo studies.

Key Message

- **U**-359 shows a significant synergistic effect in combination with Tx.
- U-359 could act synergistically with Tx in order to down-regulate the level of TUBIII and Nlp proteins.

- U-359 prevents the development of Tx resistance in MCF-7 cells causing alterations in microtubule dynamics and changes in microtubules' stabilization.

Data Sharing Statement

All materials are available.

Consent for Publication

All authors have agreed to publish this manuscript.

Funding

The present study was supported by grant Preludium No. DEC-2017/25/N/NZ3/01039 to A.D-P from the National Science Center (NCN).

Disclosure

The authors have no relevant financial or non-financial interests to disclose.

References

1. Sung H, Ferlay J, Siegel RL, et al. Global cancer statistics 2020: GLOBOCAN estimates of incidence and mortality worldwide for 36 cancers in 185 countries. *CA: Cancer J Clin*. 2021;71(3):209–249. doi:10.3322/caac.21660
2. Gallego-Jara J, Lozano-Terol G, Sola-Martínez RA, Cánovas-Díaz M, de Diego Puente T. A compressive review about taxol: History and future challenges. *Molecules*. 2020;25(24):1–24. doi:10.3390/molecules25245986
3. Haggag Y, Abu Ras B, El-Tanani Y, et al. Co-delivery of a RanGTP inhibitory peptide and doxorubicin using dual-loaded liposomal carriers to combat chemotherapeutic resistance in breast cancer cells. *Expert Opin Drug Deliv*. 2020;17(11):1655–1669.
4. Haggag YA, Yasser M, Tambuwala MM, El Tokhy SS, Isreb M, Donia AA. Repurposing of Guanabenz acetate by encapsulation into long-circulating nanopolymersomes for treatment of triple-negative breast cancer. *Int J Pharm*. 2021;600:120532.
5. Wani MC, Taylor HL, Wall ME, Coggon P, McPhail A. Plant antitumour agents VI. The isolation and structure of taxol, a novel antileukemic and antitumor agent agent from Taxus brevifolia. *J Am Chem Soc*. 1971; 93:2325–2327.
6. Xiao H, Verdier-Pinard P, Fernandez-Fuentes N, et al.Insights into the mechanism of microtubule stabilization by Taxol. *Proc Natl Acad Sci USA*. 2006;103(27):10166–10173. doi:10.1073/pnas.0603704103
7. Bukowski K, Kciuk M, Kontek R. Mechanisms of multidrug resistance in cancer chemotherapy. *Int J Mol Sci*. 2020;21(9):1–24. doi:10.3390/ijms21093233
8. Saloustros E, Mavroudis D, Georgoulias V. Paclitaxel and docetaxel in the treatment of breast cancer. *Expert Opin Pharmacother*. 2008;9(15):2603–2616. doi:10.1517/14656566.9.15.2603
9. Orr GA, Verdier-Pinard P, McDaid H, Horwitz SB. Mechanisms of Taxol resistance related to microtubules. *Oncogene*. 2003;22(47):7280–7295. doi:10.1038/SJ.ONC.1206934
10. Liverani C, De Vita A, Spadazzi C, et al. Lineage-specific mechanisms, and drivers of breast cancer chemoresistance revealed by 3D biomimetic culture. *Mol Oncol*. 2022;16(4):921–939.
11. Luo X, Wang G, Wang Y, et al. Gibberellin derivative GA-13315 overcomes multidrug resistance in breast cancer by up-regulating BMP6 expression. *Front Pharmacol*. 2022;13:1059365.
12. Długosz A, Janecka A. ABC transporters in the development of multidrug resistance in cancer therapy. *Curr Pharm Design*. 2016;22:4705–4716. doi:10.2174/1381612822666160302103646
13. Cabral F. Mechanisms of resistance to drugs that interfere with microtubule assembly. The Role of Microtubules in Cell Biology. *Neuro Oncol*. 2008;2008:337–356.
14. Hari M, Loganzo F, Annable T, et al. Paclitaxel-resistant cells have a mutation in the paclitaxel-binding region of β-tubulin (Asp26Glu) and less stable microtubules. *Mol Cancer Ther*. 2006;5(2):270–278. doi:10.1158/1535-7163.MCT-05-0190
15. Wang Y, Yin S, Blade K, Cooper G, Menick DR, Cabral F. Mutations at Leucine 215 of β-tubulin affect paclitaxel sensitivity by two distinct mechanisms. *Biochemistry*. 2006;45(1):185–194. doi:10.1021/bi051207d
16. Yin S, Bhattacharya R, Cabral F. Human mutations that confer paclitaxel resistance. *Mol Cancer Ther*. 2010;9(2):327–335. doi:10.1158/1535-7163.MCT-09-0674
17. Myers AJ, Pittman AM, Zhao AS, et al.The MAPT H1c risk haplotype is associated with increased expression of tau and especially of 4 repeat containing transcripts. *Neurobiol Dis*. 2007;25(3):561–570. doi:10.1016/j.nbd.2006.10.018
18. Rouzier R, Rajan R, Wagner P, et al. Microtubule-associated protein tau: a marker of paclitaxel sensitivity in breast cancer. *Proc Natl Acad Sci USA*. 2005;102(23):8315–8320. doi:10.1073/pnas.0408974102
19. Berruti A, Bitossi R, Gorzegno G, et al. Paclitaxel, vinorelbine and 5-fluorouracil in breast cancer patients pretreated with adjuvant anthracyclines. *Br J Cancer*. 2005;92(4):634–638. doi:10.1038/sj.bjc.6602335
20. Dean JL, McClendon AK, Knudsen ES. Modification of the DNA damage response by therapeutic CDK4/6 inhibition. *J Biol Chem*. 2012;287:29075–87.
21. Pięta M, Kędzia J, Kowalczyk D, Wojciechowski J, Wolf WM, Janecki T. Enantioselective synthesis of 5-methylidenedihydrouracils as potential anticancer agents. *Tetrahedron*. 2019;75:2495–2250. doi:10.3390/molecules25030611

22. Długosz-Pokorska A, Drogosz J, Pięta M, et al. New uracil analogs with exocyclic methylidene group as potential anticancer agents. *Anticancer Agents Med Chem*. 2020;20(3):359–368. doi:10.2174/1871520619666191211104128
23. Mosmann T. Rapid colorimetric assay for cellular growth and survival: application to proliferation and cytotoxicity assays. *J Immunol Methods*. 1983;65(1–2):55–63. doi:10.1016/0022-1759(83)90303-4
24. Winer J. Development and validation of real-time quantitative reverse transcriptase–polymerase chain reaction for monitoring gene expression in cardiac myocytesin vitro. *Anal Biochem*. 1999;41–49. doi:10.1006/abio.1999.4085
25. Foucquier J, Guedj M. Analysis of drug combinations: current methodological landscape. *Pharmacol Res Perspect*. 2015;3(3):e00149. doi:10.1002/prp2.149
26. Anampa J, Makower D, Sparano JA. Progress in adjuvant chemotherapy for breast cancer: an overview. *BMC Medic*. 2015;13(1):2–13. doi:10.1186/s12916-015-0439-8
27. Fisusi FA, Akala EO. Drug combinations in breast cancer therapy. *Pharm Nanotech*. 2019;7(1):3–23. doi:10.2174/2211738507666190122111224.
28. Sun Y, Kumar P, Sodani K, et al. Ponatinib enhances anticancer drug sensitivity in MRP7-overexpressing cells. *Oncol Rep*. 2014;31(4):1605–1612. doi:10.3892/or.2014.3002
29. Motiwala MN, Rangari VD. Combined effect of paclitaxel and piperine on an MCF-7 breast cancer cell line in vitro: Evidence of a synergistic interaction. *Synergy*. 2015;2(1):1–6. doi:10.1016/j.synres.2015.04.001
30. Tian W, Liu J, Guo Y, Shen Y, Zhou D, Guo S. Self-assembled micelles of amphiphilic PEGylated rapamycin for loading paclitaxel and resisting multidrug resistant cancer cells. *J Mater Chem*. 2015;3(7):1204–1207. doi:10.1039/c4tb01633e
31. Yang X, Shen J, Gao Y, et al. Nsc23925 prevents the development of paclitaxel resistance by inhibiting the introduction of P-glycoprotein and enhancing apoptosis. *Int J Cancer Res*. 2015;137(8):2029–2039. doi:10.1002/ijc.29574